

# Optimized Vehicle-Specific Trajectories for Cooperative Process Estimation by Sensor-Equipped UAVs\*

Juliane Euler<sup>1</sup> and Oskar von Stryk<sup>1</sup>

**Abstract**—This paper presents a sequential optimum design approach for estimating the parameters of an atmospheric dispersion process model based on measurement data gathered by a team of cooperating sensor-equipped UAVs. Locally optimal waypoint sequences that account for each UAV's possibly heterogeneous motion dynamics are computed by minimizing a suitable optimality criterion. Following these waypoints, the UAVs cooperatively maximize the information gain of the acquired measurements. A decentralized data-driven online control scheme is proposed that couples parameter estimation, waypoint calculation, and vehicle control and enables the UAVs to adaptively observe the dynamic process and iteratively improve the parameter estimate.

Simulations demonstrate the effectiveness of the proposed scheme in reducing the error between the estimated and the true dispersion model parameters compared to non-adaptive sensing strategies. In addition, the effect of using different optimality criteria, different numbers and types of UAVs as well as two options for decentralizing the waypoint calculation are investigated.

## I. INTRODUCTION

Monitoring the atmospheric dispersion of volcanic ash and radioactive or otherwise hazardous airborne material is a typical non-visual remote sensing application for unmanned aerial vehicles (UAVs). These phenomena represent large-scale dynamic spatio-temporal processes that can hardly be captured by stationary sensor networks. Sensor-carrying UAVs, instead, can be deployed flexibly and move to the most relevant measurement locations. This paper investigates cooperative sensing by multiple UAVs for the purpose of estimating the parameters of an atmospheric dispersion model.

The efficiency of the measurement process can be maximized using an adaptive control approach that accounts for already available information as well as the UAVs' individual physical capabilities. This can be achieved by not only incorporating new measurement data to update the parameter estimate, but by feeding the estimate back to the UAVs' motion controller in a way that the information gain of future measurements is maximized. This closed loop between application and measurements is characteristic for so called *Dynamic Data Driven Application Systems* (DDDAS) [1].

Model-based DDDAS in the context of atmospheric dispersion monitoring can be implemented in many different ways: In [2], the authors utilize virtual attractor particles to guide multiple UAVs collecting data for a pollutant puff simulation. A loss function combining misclassification and

mutual information is minimized in [3] to choose the best option from a finite set of possible actions for each UAV. This is similarly done in [4] and [5], where a measure for the uncertainty of the parameter estimate is optimized instead. Above approaches, however, do not explicitly incorporate the UAVs' motion dynamics.

The authors of [6] do so by optimizing a set of waypoint sequences that maximize the forecast accuracy of a PDE plume model subject to the vehicle dynamics. The data-driven scheme proposed in [7] is also based on a PDE process model and the Ensemble Kalman Filter, but combines it with a separate model-predictive cooperative controller. Since PDE-based simulations are computationally intensive, both approaches depend on a central computing unit.

[8] provides a comprehensive theoretical background on optimum design for identifying distributed parameter systems. Here, the goal is to solve a complex optimal control problem (OCP) that minimizes an optimality criterion subject to ordinary differential equations representing the vehicle dynamics. A similar idea is also pursued in [9]. However, online adaptability of the vehicles' motion to the gathered information is not possible in these feedforward approaches and solving the OCP quickly becomes computationally intensive. In order to overcome these drawbacks, the OCP can repeatedly be solved in a receding horizon fashion, as proposed in [10] and [11]. The feedback loop can be closed that way, but both approaches [10], [11] depend on a central instance able to solve the OCP. As communication between the central instance and the UAVs is likely to be limited, decentralized solutions are preferable for real-world applications and offer the additional benefit of being scalable to larger UAV teams.

In this paper, the DDDAS scheme is implemented as sequential optimum design approach. By minimizing a suitable optimality criterion, sequences of spatiotemporal waypoints are determined, where measurements collected by sensor-equipped UAVs are most valuable for improving the parameter estimate of a Gaussian puff model. The design problem is constrained by the UAVs' (possibly heterogeneous) motion dynamics and therefore provides vehicle-specific locally optimal waypoint sequences as input for each UAV's motion controller. Parameter estimation (Sec. II), waypoint calculation (Sec. III), and vehicle control permanently interact as illustrated in Fig. 1. By coupling the estimation and the control problem in that way, an efficient decentralized data-driven online control scheme is obtained.

\*This research has been supported in parts within the Hessian LOEWE initiative by the NICER project.

<sup>1</sup> Department of Computer Science, Technische Universität Darmstadt, Germany, {euler, stryk}@sim.tu-darmstadt.de

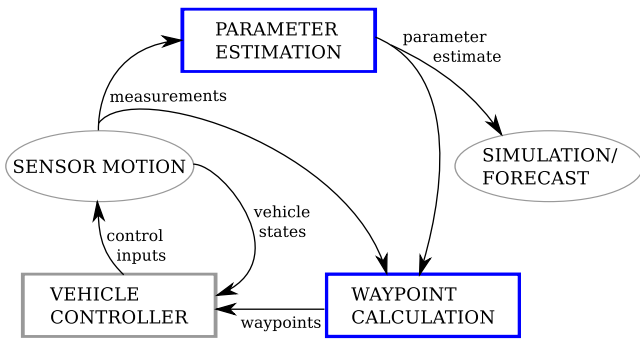


Fig. 1. Schematic view of the proposed dynamic data-driven sensing loop. The focus of this paper is on the interaction of the elements PARAMETER ESTIMATION and WAYPOINT CALCULATION highlighted in blue.

## II. DISPERSION MODEL

Gas emissions in the atmosphere can be described by the advection-diffusion equation

$$\frac{\partial C}{\partial t} = -\nabla \cdot \mathbf{q}, \quad (1)$$

where  $C(\mathbf{x}, t)$  is the contaminant concentration in  $[\text{kg}/\text{m}^3]$  at location  $\mathbf{x} \in \mathbb{R}^3$  at time  $t$  and  $\mathbf{q}$  is the mass flux in  $[\text{kg}/\text{m}^2\text{s}]$ .  $\mathbf{q}$  combines diffusion and advection since

$$\mathbf{q} = \mathbf{q}_A + \mathbf{q}_D = C\mathbf{v}_w - \mathbf{K}\nabla C, \quad (2)$$

where  $\mathbf{v}_w$  is the wind velocity in  $[\text{m}/\text{s}]$ ,  $\mathbf{K} = \text{diag}(K_x, K_y, K_z)$  is the diffusion coefficient, and  $K_x(\mathbf{x}), K_y(\mathbf{x}), K_z(\mathbf{x})$   $[\text{m}^2/\text{s}]$  turbulent eddy diffusivities.

### A. Solving the Advection-Diffusion Equation

Under a number of simplifying assumptions (detailed in [12]), by Laplace transform one can obtain

$$C(\boldsymbol{\theta}, x, y, z, t) = \frac{Q}{8\pi^{\frac{3}{2}}(K_x K_y K_z)^{\frac{1}{2}} \Delta t^{\frac{3}{2}}} \cdot e^{-\frac{(\Delta x - u \Delta t)^2}{4K_x \Delta t} - \frac{\Delta y^2}{4K_y \Delta t}} \cdot \left( e^{-\frac{(z - z_0)^2}{4K_z \Delta t}} + e^{-\frac{(z + z_0)^2}{4K_z \Delta t}} \right), \quad (3)$$

as the so called *Gaussian puff solution* of (1). Here,  $Q$   $[\text{kg}]$  is the total mass of the instantaneous release,  $(x_0, y_0, z_0)$  is the location of the source in  $[\text{m}]$ ,  $t_0$   $[\text{s}]$  the time of the release,  $\Delta x = x - x_0$ ,  $\Delta y = y - y_0$ ,  $\Delta t = t - t_0$ , and  $\mathbf{v}_w = (u, 0, 0)$ .

Further assuming that the lateral eddy diffusion in  $x$  and  $y$  direction is identical, i.e.  $K_x = K_y$ , and that  $K_z$  can be derived from the theoretical model  $K_z = a(z - z_0)^n$  [12] with  $a$  and  $n$  depending on the atmospheric conditions, the vector of unknown parameters for the Gaussian puff solution (3) is  $\boldsymbol{\theta} = (Q, K_x, x_0, y_0, z_0, t_0)^T$ .

The Gaussian model is used extensively as the standard approach in literature studying industrial emissions, various pollutant transport processes as well as the release of nuclear or biological contaminants [13]. For the latter case, the importance of (Gaussian) dispersion models that offer “a quick, simple, hands-on prediction capability for plume direction, coverage, and lethality” for first responders is emphasized in [14]. However, the approach presented in the following

section could equally well deal with other analytical solutions of (1). It is possible to extend the Gaussian solutions to represent more complex dispersion phenomena, e.g. multiple sources or stronger turbulences. In general, more complex solutions of (1) can be derived by changing the underlying assumptions and boundary conditions (cf. [13]).

### B. Parameter Estimation Problem

Let  $(\mathbf{p}_i, v_i)$ ,  $i = 1, 2, \dots, m$ , be  $m$  data points with measurements  $v_i$  defined as

$$v_i = C_i(\boldsymbol{\theta}_{\text{true}}) + \epsilon_i, \quad i = 1, 2, \dots, m, \quad (4)$$

where  $C_i(\boldsymbol{\theta}_{\text{true}}) = C(\boldsymbol{\theta}_{\text{true}}, \mathbf{p}_i)$  as defined in (3) and  $\boldsymbol{\theta}_{\text{true}}$  is the true parameter vector to be estimated.  $\mathbf{p}_i = (x_i, y_i, z_i, t_i)$  contains the coordinates of the  $i$ th measurement in space and time. The measurement error  $\epsilon_i$  is assumed to be white Gaussian noise with mean  $\mathbb{E}(\epsilon_i) = 0$  and variance  $\text{var}(\epsilon_i) = \sigma_i^2$ . Following the problem definition in [5], the standard deviation  $\sigma_i$  of the error is modeled as  $\sigma_i = \frac{v_i}{\alpha}$  with a constant signal to noise ratio (SNR)  $\alpha^2 = 1000$ . It is further assumed that the measurement errors are uncorrelated, i.e.  $\mathbb{E}(\epsilon_i \epsilon_j) = \text{cov}(\epsilon_i, \epsilon_j) = 0$  for  $i \neq j$ .

The following *weighted nonlinear least squares* problem is solved to estimate the parameter vector  $\boldsymbol{\theta}$ :

$$\min_{\boldsymbol{\theta}} \frac{1}{2} \|\mathbf{W}(\mathbf{v} - \mathbf{C}(\boldsymbol{\theta}))\|_2^2. \quad (5)$$

Here,  $\mathbf{v} = (v_1, v_2, \dots, v_m)^T$  and  $\mathbf{C}(\boldsymbol{\theta}) = (C_1(\boldsymbol{\theta}), C_2(\boldsymbol{\theta}), \dots, C_m(\boldsymbol{\theta}))^T$ . Since the standard deviations of the measurement errors are not identical, each residual  $v_i - C_i(\boldsymbol{\theta})$  needs to be weighted by the reciprocal of  $\sigma_i$ . Hence,  $\mathbf{W} = \text{diag}(\sigma_1^{-1}, \sigma_2^{-1}, \dots, \sigma_m^{-1}) \in \mathbb{R}^{m \times m}$ .

In order to most efficiently obtain an accurate estimate of the parameters  $\boldsymbol{\theta}$  of the Gaussian puff model (3), the sensor UAVs are to collect measurements  $v_i$  at locations where maximum information gain and, hence, maximum improvement of the solution of problem (5) can be expected. Identifying these optimum locations respecting previously gathered information as well as the vehicles’ motion capabilities is subject of the following section.

## III. WAYPOINTS FOR OPTIMAL SENSING

### A. UAV Dynamics

Quadrotor as well as fixed-wing UAVs are considered as sensor platforms in this paper. The modeling of their motion dynamics is described in the following.

a) *Quadrotor UAV*: Quadrotor UAVs are modeled as point mass with double integrator dynamics  $\dot{\mathbf{x}} = \mathbf{u}$  [15], i.e. the first order ODE describing the motion dynamics is

$$\dot{\mathbf{x}}_{qr} = \begin{pmatrix} v_x \\ v_y \\ v_z \\ u_x \\ u_y \\ u_z \end{pmatrix} = \mathbf{f}_{qr}(\mathbf{x}_{qr}, \mathbf{u}_{qr}), \quad (6)$$

where the state vector  $\mathbf{x}_{qr} = (x, y, z, v_x, v_y, v_z)^T$  contains the quadrotor's x/y/z positions and velocities, and the vector of control inputs  $\mathbf{u}_{qr} = (u_x, u_y, u_z)^T$  comprises its x/y/z accelerations. Euler discretization of (6) yields

$$\mathbf{x}_{qr}^{k+1} = \mathbf{x}_{qr}^k + \Delta t \cdot \mathbf{f}_{qr}(\mathbf{x}_{qr}^k, \mathbf{u}_{qr}^k), \quad (7)$$

where  $\Delta t$  is the step size and the superscript  $k$  relates to the time step  $t_k = k \cdot \Delta t$ .

b) *Fixed-Wing UAV*: A simple airplane model (cf. [15]) is used to describe the motion of fixed-wing UAVs:

$$\dot{\mathbf{x}}_{fw} = \begin{pmatrix} s \cdot \cos \varphi \\ s \cdot \sin \varphi \\ v_z \\ \omega_\varphi \\ u_z \\ u_\omega \end{pmatrix} = \mathbf{f}_{fw}(\mathbf{x}_{fw}, \mathbf{u}_{fw}). \quad (8)$$

Here, the state vector  $\mathbf{x}_{fw} = (x, y, z, \varphi, v_z, \omega_\varphi)^T$  contains the UAV's x/y/z position, orientation  $\varphi$ , climb/descent rate  $v_z$ , and angular velocity  $\omega_\varphi$ . Control inputs  $\mathbf{u}_{fw} = (u_z, u_\omega)^T$  are the climb/descent acceleration  $u_z$  and the angular acceleration  $u_\omega$ . A constant forward speed  $s = \text{const}$  is assumed. Takeoff and landing of the aircraft are not modeled. Euler discretization of (8) yields

$$\mathbf{x}_{fw}^{k+1} = \mathbf{x}_{fw}^k + \Delta t \cdot \mathbf{f}_{fw}(\mathbf{x}_{fw}^k, \mathbf{u}_{fw}^k). \quad (9)$$

Although wind velocity is an important parameter of the Gaussian puff model, both UAV dynamics models do not account for the influence of wind. It is assumed that the UAVs' motion controller is able to compensate wind disturbances at least for the low winds considered in this paper. This justifies the calculation of waypoints neglecting the impact of wind on the UAVs' flight paths. For dealing with stronger winds, they could be incorporated also in the UAV dynamics models.

### B. Optimum Design Problem

Let  $\bar{\boldsymbol{\theta}}$  be the result of the parameter estimation problem (5). Since the Gaussian puff model (3) is nonlinear in the parameters  $\boldsymbol{\theta}$ , an optimum design will depend on these parameters and, thus, on the quality of the estimate  $\bar{\boldsymbol{\theta}}$ . In order to compensate negative effects of bad estimates  $\bar{\boldsymbol{\theta}}$  on the design, a sequential design approach [16] is employed in this paper. In a first step, a linearization of the Gaussian puff model (3) by Taylor series expansion about  $\bar{\boldsymbol{\theta}}$  combining all available measurement data yields

$$\mathbf{C}(\boldsymbol{\theta}) = \mathbf{C}(\bar{\boldsymbol{\theta}}) + \mathbf{J}_C \cdot (\boldsymbol{\theta} - \bar{\boldsymbol{\theta}}), \quad (10)$$

where the Jacobian of  $\mathbf{C}(\bar{\boldsymbol{\theta}})$  denoted as

$$\begin{aligned} \mathbf{J}_C &= (\nabla C_1(\bar{\boldsymbol{\theta}}), \nabla C_2(\bar{\boldsymbol{\theta}}), \dots, \nabla C_m(\bar{\boldsymbol{\theta}}))^T \\ &= (\nabla C(\bar{\boldsymbol{\theta}}, \mathbf{p}_1), \nabla C(\bar{\boldsymbol{\theta}}, \mathbf{p}_2), \dots, \nabla C(\bar{\boldsymbol{\theta}}, \mathbf{p}_m))^T \end{aligned}$$

is the *extended design matrix* for the linearized model ( $C$  as defined in (3)). From that, the *information matrix*

$$\mathbf{M} = \mathbf{J}_C^T \mathbf{W}^2 \mathbf{J}_C \quad (11)$$

is obtained.  $\mathbf{W}$  is the same as in (5). In order to determine an optimum design for the linearized model (i.e. optimized

new measurement locations  $\tilde{\mathbf{p}}_{v,1}, \dots, \tilde{\mathbf{p}}_{v,n_w}$  as waypoints for each UAV  $v$ ),  $\mathbf{M}$  is extended such that

$$\begin{aligned} \mathbf{M}_{\text{ext}} &= \mathbf{M} + \nabla C(\bar{\boldsymbol{\theta}}, \tilde{\mathbf{p}}_{v,1}) \nabla C(\bar{\boldsymbol{\theta}}, \tilde{\mathbf{p}}_{v,1})^T + \\ &\quad \dots + \nabla C(\bar{\boldsymbol{\theta}}, \tilde{\mathbf{p}}_{v,n_w}) \nabla C(\bar{\boldsymbol{\theta}}, \tilde{\mathbf{p}}_{v,n_w})^T \end{aligned} \quad (12)$$

for all UAVs  $v = 1, 2, \dots, n_w$ . That way,  $\mathbf{M}_{\text{ext}}$  becomes dependent on the waypoints to be determined. The volume of the confidence ellipsoid of the parameters  $\bar{\boldsymbol{\theta}}$  is inversely proportional to  $\sqrt{\det(\mathbf{M}_{\text{ext}})}$ . Hence, it is desirable to maximize  $\det(\mathbf{M}_{\text{ext}})$  in order to improve the reliability of the parameter estimate. This leads to the so called *D-optimality* criterion [16], a convex formulation of which is

$$\Psi_D(\mathbf{M}_{\text{ext}}) = -\log(\det(\mathbf{M}_{\text{ext}})). \quad (13)$$

Other frequently used optimality criteria expressed in terms of the eigenvalues  $\lambda_i$  of  $\mathbf{M}_{\text{ext}}$  are *A-optimality*

$$\Psi_A(\mathbf{M}_{\text{ext}}) = \prod_i \frac{1}{\lambda_i} \quad (14)$$

corresponding to the diagonal of the bounding box of the confidence ellipsoid and *E-optimality*

$$\Psi_E(\mathbf{M}_{\text{ext}}) = \max_i \frac{1}{\lambda_i} \quad (15)$$

corresponding to the largest radius of the confidence ellipsoid [16]. Minimization of one of the optimality criteria subject to the UAVs' motion dynamics models leads to the following design problem for the determination of optimized vehicle-specific waypoint sequences:

$$\min_{\tilde{\mathbf{p}}_{v,1}, \tilde{\mathbf{p}}_{v,2}, \dots, \tilde{\mathbf{p}}_{v,n_w}} \Psi(\mathbf{M}_{\text{ext}} + \mu \mathbf{I}) \quad (16a)$$

$$\text{s.t.} \quad \mathbf{x}^{k+1} = \mathbf{x}^k + \Delta t \cdot \mathbf{f}(\mathbf{x}^k, \mathbf{u}^k) \quad (16b)$$

$$\tilde{\mathbf{p}}_{v,k+1} = \mathbf{C}_v \mathbf{x}^{k+1} \quad (16c)$$

$$\mathbf{x}_{\min} \leq \mathbf{x}^k \leq \mathbf{x}_{\max} \quad (16d)$$

$$\mathbf{u}_{\min} \leq \mathbf{u}^k \leq \mathbf{u}_{\max}, \quad (16e)$$

where  $k = 0, 1, \dots, n_w - 1$ . Constraint (16b) represents the dynamics of all  $n_w$  UAVs considered in the problem since

$$\mathbf{x}^k = \begin{pmatrix} \mathbf{x}_1^k \\ \vdots \\ \mathbf{x}_{n_w}^k \end{pmatrix}, \mathbf{u}^k = \begin{pmatrix} \mathbf{u}_1^k \\ \vdots \\ \mathbf{u}_{n_w}^k \end{pmatrix}, \mathbf{f}(\mathbf{x}^k, \mathbf{u}^k) = \begin{pmatrix} \mathbf{f}(\mathbf{x}_1^k, \mathbf{u}_1^k) \\ \vdots \\ \mathbf{f}(\mathbf{x}_{n_w}^k, \mathbf{u}_{n_w}^k) \end{pmatrix},$$

where  $\mathbf{x}_v, \mathbf{u}_v, \mathbf{f}_v$  correspond to the type of UAV  $v$ . Constraint (16c) is not implemented, but stated here to illustrate the extraction of waypoints from the overall vehicle state vector. The term  $\mu \mathbf{I}$  with small  $\mu$  is required to regularize the information matrix. The software package SNOPT 7.5 [17] is employed to solve the nonlinear program (NLP) (16).

The waypoints can be tailored to the current or a predicted vehicle state by selecting the initial value  $\mathbf{x}_v^0$  accordingly. This allows collateral precalculation of new waypoints while the sensor vehicle is still collecting data along previously determined waypoints.

Whenever additional measurement data has been gathered, it can be incorporated to obtain an updated parameter estimate  $\bar{\boldsymbol{\theta}}$  from (5). Based on the new  $\bar{\boldsymbol{\theta}}$ , the linearization (10) can be recalculated and the sequential design restarts.

### C. Decentralized Waypoint Calculation

Our high-level objective is the development of a fully decentralized dynamic data-driven control loop for cooperative process estimation by multiple UAVs as depicted in Fig. 1. Therefore, all loop components including PARAMETER ESTIMATION and WAYPOINT CALCULATION have to be performed by each UAV individually. For this purpose, it is assumed that the UAVs exchange the measurement data they gathered, their current parameter estimate  $\hat{\theta}$  as well as their current state vector whenever they are within communication range to each other.

Two options can be considered for the way a UAV calculates its waypoint sequences.

*Option 1:* Problem (16) is set up only for the UAV itself, i.e. constraint (16b) contains only one motion dynamics model and only one waypoint sequence is determined. That way, each UAV will try to improve the parameter estimate without considering its teammates' actions.

*Option 2:* Problem (16) is set up for the UAV itself plus all teammates within communication range. From the resulting waypoint sequences only the calculating UAV's own sequence is actually used. This joint waypoint calculation can be assumed to result in better cooperative behavior than Option 1 since the optimization accounts also for the teammates' (potential) future measurements.

It is obvious that the NLP for the joint waypoint calculation in Option 2 is more complex and its solution therefore more time consuming than Option 1. The differences in the UAVs' behavior and the quality of the parameter estimate resulting from the two different options will be evaluated in Sec. IV-C.

## IV. EVALUATION

Purpose of the following analysis is to prove the general effectiveness of the waypoint approach with respect to the quality of the resulting parameter estimate. This is done under idealized conditions omitting inaccuracies stemming from the deviation between the motion dynamics models in problem (16) and the actual UAV motion. That means, the vehicle controller step in the data-driven sensing loop (Fig. 1) is skipped and the sensors are assumed to collect measurements precisely at the calculated spatio-temporal locations. Moreover, perfect communication is assumed, making identical measurement data and parameter estimates available to all UAVs at any time. Measurement noise is the only considered error source (cf. Sec. II-B).

### A. Comparison of Optimality Criteria

In Sec. III-B, the criteria for A-, D-, and E-optimality were introduced. From a theoretical point of view, D-optimality has a significant advantage over the other two criteria as it is invariant to affine transformations of  $\nabla C(\theta, \mathbf{p})$ . Hence, changing a unit of measure, e.g. from [m] to [cm], would not affect the D-optimum design. In order to evaluate differences in the performance of the proposed waypoint approach with respect to the employed optimality criterion, a set of 60 simulation runs per criterion was performed.

TABLE I

SIMULATION PARAMETERS		
parameter	value	unit
domain size	$F = 500$	[m]
min UAV altitude	$z_{\min} = 5$	[m]
initial UAV positions	$\mathbf{x}_1^0 = (-50, 0, 5)$ $\mathbf{x}_2^0 = (-50, -50, 5)$ $\mathbf{x}_3^0 = (-50, 50, 5)$	[m]
sensing rate	$\Delta t = 2$	[s]
true puff parameters	$\theta_{\text{true}} = \begin{pmatrix} Q \\ K_x \\ x_0 \\ y_0 \\ z_0 \\ t_0 \end{pmatrix} = \begin{pmatrix} 1000 \\ 12 \\ 2 \\ 5 \\ 0 \\ 0 \end{pmatrix}$	$\begin{pmatrix} [\text{kg}] \\ [\text{m}^2/\text{s}] \\ [\text{m}] \\ [\text{m}] \\ [\text{m}] \\ [\text{s}] \end{pmatrix}$
initial estimate	$\bar{\theta}_0 = \begin{pmatrix} Q \\ K_x \\ x_0 \\ y_0 \\ z_0 \\ t_0 \end{pmatrix} = \begin{pmatrix} 700 \\ 20 \\ 40 \\ 25 \\ 1 \\ 30 \end{pmatrix}$	$\begin{pmatrix} [\text{kg}] \\ [\text{m}^2/\text{s}] \\ [\text{m}] \\ [\text{m}] \\ [\text{m}] \\ [\text{s}] \end{pmatrix}$
diffusivity parameter	$K_z = 0.2113$	$[\text{m}^2/\text{s}]$
<b>quadrotor UAV</b>		
max x/y/z velocity	$v_{\max} = 10$	[m/s]
max x/y/z acceleration	$u_{\max} = 3$	$[\text{m}/\text{s}^2]$
<b>fixed-wing UAV</b>		
max z velocity	$v_{z\max} = 2$	[m/s]
max ang. velocity	$\omega_{\varphi\max} = 9$	[deg/s]
max z acceleration	$v_{z\max} = 0.16$	$[\text{m}/\text{s}^2]$
max ang. acceleration	$u_{\varphi\max} = 0.3$	$[\text{deg}/\text{s}^2]$
forward speed	$s = 18$	[m/s]

All values of the variables mentioned in the following are given in Table I. On a  $[-F, F] \times [-F, F] \times [0, 50] \subset \mathbb{R}^3$  domain, a Gaussian puff with parameters  $\theta_{\text{true}}$  is to be identified. With the joint waypoint calculation approach as introduced in Sec. III-C and each of the criteria (14), (13), and (15), sequences of  $n_w = 4$  waypoints per optimization are generated for  $n_v = 1/2/3$  quadrotor UAVs starting at the initial positions  $\mathbf{x}_{1/2/3}^0$ . The last waypoint of the previous sequence serves as starting point for the next waypoint sequence. In order to guarantee that a feasible follow-up sequence exists, 4+2=6 waypoints are determined per optimization, but only the first 4 are actually used. The UAVs start at time  $t = 100$  and take measurements every  $\Delta t$  s. Measurement noise is modeled as described in Sec. II-B and the wind conditions were uniformly varied between  $u \in \{0.5, 0, -0.5, 1\}$ . The initial parameter estimate  $\bar{\theta}_0$  is assumed to be updated every  $\Delta t$  s and the sequence of estimates over a period of 50 s was evaluated.

Fig. 2 shows the resulting root mean squared error (RMSE) for the different criteria and numbers of UAVs  $n_v$ . It reveals, that in terms of the RSME, E-optimality performs significantly worse than A- and D-optimality. They provide very similar estimate accuracies for all numbers of UAVs, D-optimality being slightly superior to A-optimality. Moreover, the different criteria perform differently in terms of the accuracies of the single parameters in  $\theta$  as shown in Fig. 2. Hence, the choice of the criterion can be made situation-dependant based on the importance of certain parameters. For the following experiments, we will employ the D-optimality criterion as it promises the best overall performance and, in addition, has the useful scaling property.

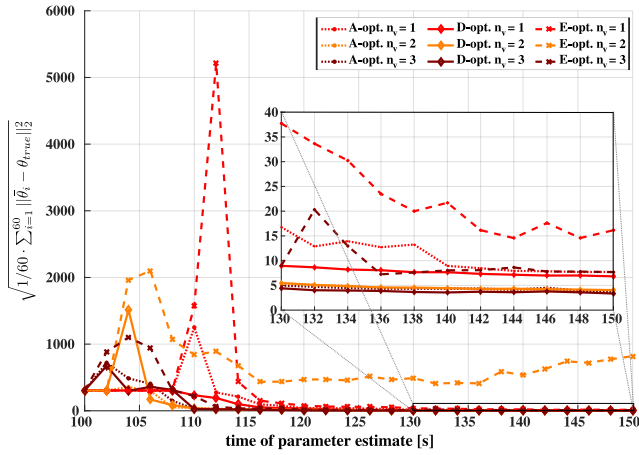


Fig. 2. RMSE in 60 simulation runs of the joint waypoint calculation approach with  $n_v = 1, 2, 3$  quadrotors employing the A-, D-, and E-optimality criterion, respectively. Wind conditions uniformly varied between  $u \in \{0.5, 0, -0.5, 1\}$  [m/s].

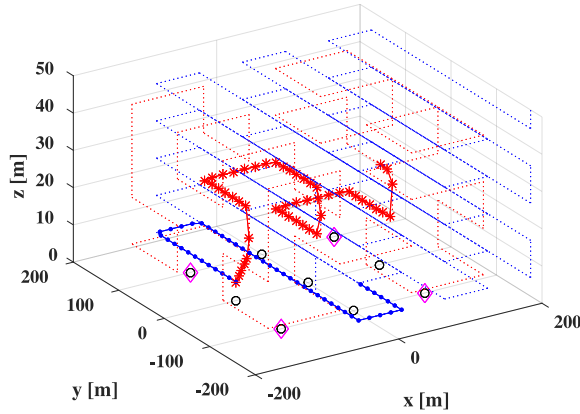


Fig. 4. Sequence of measurement locations resulting from wavy line motion (blue  $\bullet$ ) and space-filling Hilbert curve motion (red  $*$ ) over a period of 50 s and  $\Delta t = 2$  s. The stationary 4-sensor network is depicted as magenta  $\diamond$ , the 9-sensor network as black  $\circ$ .

### B. Comparison to Motion Patterns and Fixed Sensors

In order to prove the effectiveness of following the optimized waypoints for maximizing the informativeness of measurements, the proposed approach is compared to two predefined sensor motion patterns as well as to two stationary sensor networks. In addition to the simulation setup described in Sec. IV-A, a single UAV following a simple wavy line motion pattern and a space-filling Hilbert curve (order  $n = 2$ ), respectively, each starting from  $\mathbf{x}_1^0$  is considered. Both patterns are illustrated in Fig. 4. In all cases, the UAVs start at time  $t = 100$  and take measurements every  $\Delta t$  s. Additionally, measurements provided from stationary sensor networks with 4 and 9 sensors, respectively, at rate  $\Delta t$  are considered. The locations of these sensors are also marked in Fig. 4. For each sensing approach, the same initial parameter estimate  $\hat{\theta}_0$  is considered and updated every  $\Delta t$  s. The resulting RMSE curves are shown in Fig. 5.

As can be seen, with respect to estimation error reduction, measurements taken at the optimized waypoints are significantly more effective than measurements taken along

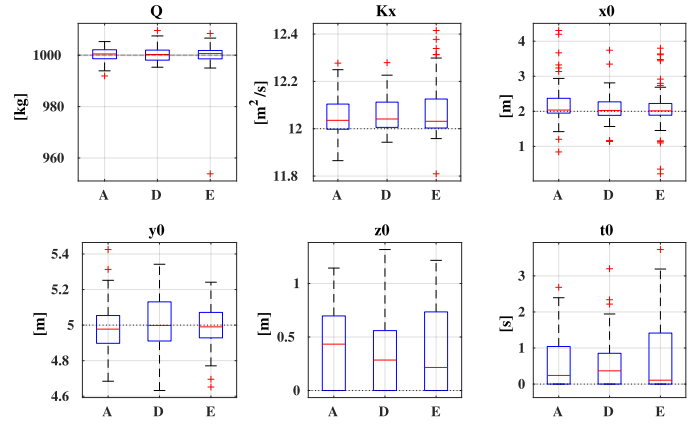


Fig. 3. Boxplots showing the estimated values of the single parameters in  $\theta$  at  $t = 150$  s in 60 simulation runs of the joint waypoint approach for  $n_v = 3$  quadrotors employing A-, D-, and E-optimality, respectively.

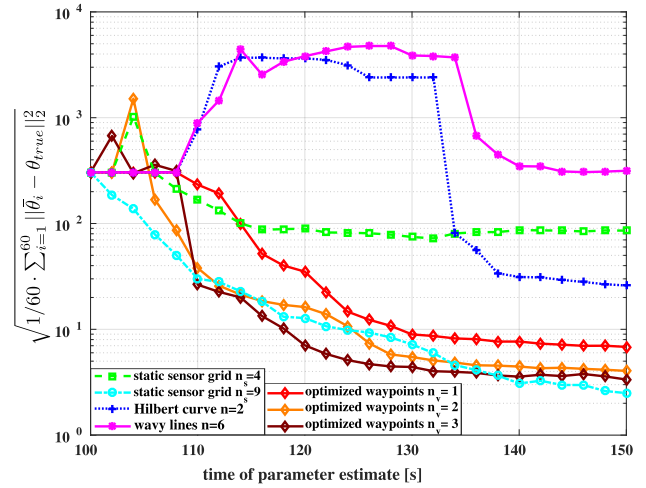


Fig. 5. RMSE in 60 simulation runs of the joint waypoint calculation with  $n_v = 1, 2, 3$  quadrotors in comparison to a single sensor moving along wavy lines and Hilbert curves as well as to two stationary sensor networks. Wind were uniformly varied between  $u \in \{0.5, 0, -0.5, 1\}$  [m/s].

predefined sensor paths. Since new waypoints are calculated every 8 s based on the current parameter estimate, the motion of the waypoint-guided UAVs adapts to the current state of the Gaussian puff. Fig. 6 shows examples of typical waypoint sequences. While the adaptive sensor motion quickly reduces the RMSE to values  $< 50$ , the wavy line motion seems to be especially disadvantageous. Since the source of the puff release is located at  $(2, 5, 0)$ , lots of measurements taken along the wavy line are located outside the puff. Hence, their information content is low, which has a strong negative influence on the parameter estimate.

For the first estimate update, corresponding to the number of unknown parameters, 6 measurements are required. This is why the curves of the wavy line, Hilbert, and waypoint-guided motion for a single UAV remain constant until enough measurements have been collected. Two and three waypoint-guided UAVs and the stationary sensor networks deliver 2/3/4/9 measurements per time step and therefore the corresponding RMSE descends earlier. As expected,

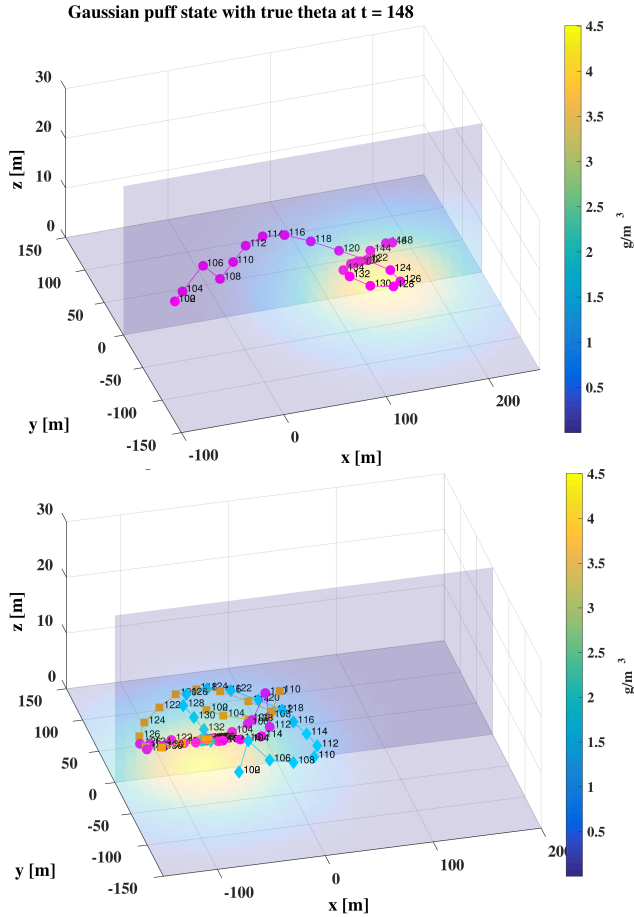


Fig. 6. Examples of optimized trajectories computed for 1 quadrotors at wind speed  $u = 1$  (top) and 3 quadrotors at  $u = -0.5$  (bottom).

the efficiency of the waypoint approach increases with the number of UAVs. In any case, the final estimation accuracy of the waypoint approach outperforms the 4-sensor network, proving that less measurements at optimized locations can be more valuable than more measurements taken at fixed positions. Also the 9-sensor network is temporarily outperformed by the waypoint approach with 3 UAVs, but eventually, the network's RMSE further decreases. This is due to the advantageous positions of the stationary sensors with respect to the puff's evolution towards the end of the simulated time period. The 9-sensor network is then able to gather 9 meaningful measurements per time step in contrast to 3 obtained from the UAVs. This could be completely different in settings where the puff cannot be covered by the fixed sensors. Then flexibly adapting UAVs are clearly in favor.

### C. Comparing Individual and Joint Waypoint Calculation

In order to compare the two waypoint calculation options introduced in Sec. III-C, 50 simulation runs for each variant were performed for 2 quadrotor UAVs. The wind speed was fixed at  $u = 0.5$ , otherwise the same simulation setup as before was used (see Table I). Figs. 7 and 8 show typical examples of waypoint sequences obtained from the joint calculation (Option 2) and the individual calculation (Option 1), respectively. Option 1 leads to an alignment of both

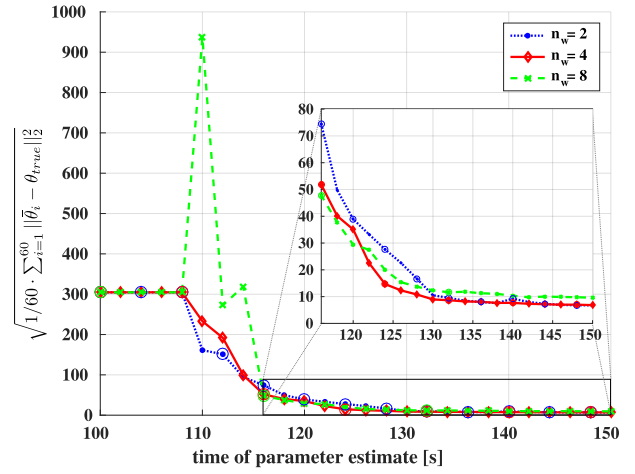


Fig. 10. RMSE in 60 simulation runs of the waypoint calculation for 1 quadrotor with  $n_w = 2, 4, 8$  waypoints per sequence. Circles indicate when new waypoints were computed.

UAV trajectories while Option 2 distributes the UAVs in the domain. Since nearly all waypoints are at  $z = 5$ , only a top down view is given. The joint calculation provides a slightly better reduction of the RMSE of the parameter estimate, the only exception being the first waypoint sequence, see Fig. 9. The average computing time (Dual Core CPU, 2.53 GHz, 8GB RAM) for one waypoint optimization accounting for both UAVs was 1.098 s, for the individual case it was 0.432 s. In a setup with 3 quadrotors, Option 2 took 4.519 s in average and the corresponding RMSE curve was even closer to that obtained with Option 1. It is left to the user to decide whether a slightly better performance of Option 2 is worth the computational effort exponentially increasing with the number of UAVs. However, Option 2 is preferable if additional constraints affecting the UAVs' cooperation, such as collision avoidance, are to be considered in the waypoint calculation. In order to still be able to scale the approach to teams with  $n_w \gg 3$  UAVs, an upper bound for the number of UAVs considered in problem (16) along with rules for their selection can be defined.

Another possibility for influencing frequency and effort of the waypoint computation is by varying the number of waypoints  $n_w$  per optimized sequence. Fig. 10 shows the RMSE performance for the simulation setup of Sec. IV-A with 1 quadrotor and  $n_w = 2/4/8$ . While  $n_w = 8$ , i.e. a recomputation interval of 16 s, does not allow good adaptation of the parameter estimate to the gathered data, a recomputation every  $n_w = 2$  waypoints seems to be too frequent since not enough relevant additional measurements can be incorporated to improve the parameter estimate. Therefore,  $n_w = 4$  appears to be a good tradeoff in terms of estimation error reduction. In terms of computational effort, the average waypoint calculation time for  $n_w = 2$  was 0.233 s, for  $n_w = 4$  it was 0.675 s, and 1.166 s for  $n_w = 8$ .

### D. Heterogeneous Teams of UAVs

The proposed waypoint approach is able to deal with heterogeneous vehicle teams as problem (16) can be modularly

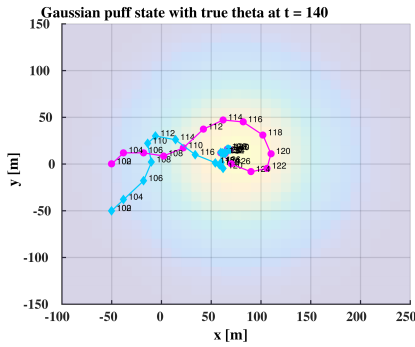


Fig. 7. Example result of a joint waypoint calculation for 2 quadrotors.

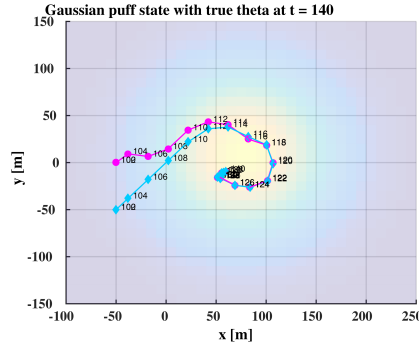


Fig. 8. Example result of an individual waypoint calculation for 2 quadrotors.

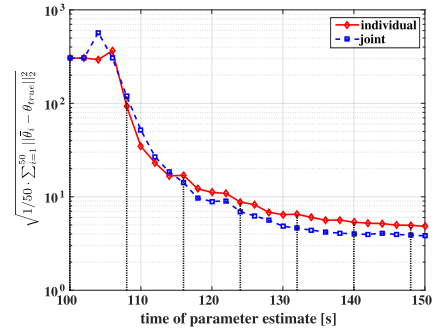


Fig. 9. RMSE resulting from individual and joint waypoint calculation. Dotted black lines indicate when waypoints were calculated.

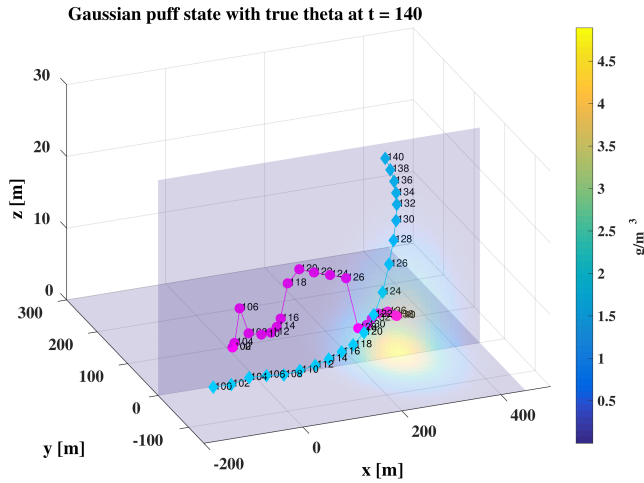


Fig. 11. Example of waypoints for a quadrotor (magenta) and a fixed-wing UAV collecting measurements at wind speed  $u = 2$  [m/s].

assembled according to the current UAV constellation. An example of waypoint sequences for a quadrotor and a fixed-wing UAV (with specification as given in Table I) is shown in Fig. 11. Due to the fixed-wing UAV's constant speed and its large turning radius, it is less agile and flexible than the quadrotor, but can quickly cover significantly larger domains. This has to be considered when both UAV type are to jointly identify a dispersion process.

## V. CONCLUSIONS

An efficient decentralized data-driven control loop for cooperating sensor-equipped UAVs was presented in this paper. Core is a novel optimum design-based approach for maximizing the informativeness of measurements by computing waypoints that are individually tailored to each vehicle and exploit the team's cooperative mobility. Simulation results illustrate the proposed approach from different perspectives and prove its effectiveness.

While this paper was intended as a general proof of concept ignoring the effects of deviations between the modeled and the actual UAV motion or limited communication, ongoing work is on investigating the waypoint approach in

a more realistic setting. It comprises the use of a model-predictive cooperative controller for guiding the UAVs along their waypoints while simultaneously allowing for additional mission objectives. By using ROS and Gazebo as implementation and simulation framework, another step is taken towards the applicability of the proposed dynamic data-driven control loop in real-world scenarios.

## REFERENCES

- [1] F. Darema, "Dynamic data driven applications systems: A new paradigm for application simulations and measurements," in *ICCS*, ser. LNCS. Springer, 2004, vol. 3038, pp. 662–669.
- [2] B. Hodgkinson, D. Lipinski, L. Peng, and K. Mohseni, "Cooperative control using data-driven feedback for mobile sensors," in *IEEE ICRA*, 2013, pp. 772–777.
- [3] V. Šmíd and R. Hofman, "Tracking of atmospheric release of pollution using unmanned aerial vehicles," *Atmospheric Environment*, vol. 67, pp. 425–436, 2013.
- [4] V. N. Christopoulos and S. Roumeliotis, "Adaptive Sensing for Instantaneous Gas Release Parameter Estimation," in *IEEE ICRA*, 2005, pp. 4450–4456.
- [5] —, "Multi Robot Trajectory Generation for Single Source Explosion Parameter Estimation," in *IEEE ICRA*, 2005, pp. 2803–2809.
- [6] D. Zhang, C. Colburn, and T. Bewley, "Estimation and adaptive observation of environmental plumes," in *ACC*, 2011, pp. 4281–4286.
- [7] J. Euler, T. Ritter, S. Ulbrich, and O. von Stryk, "Centralized Ensemble-Based Trajectory Planning of Cooperating Sensors for Estimating Atmospheric Dispersion Processes," in *Dynamic Data-Driven Environmental Systems Science*, 1st ed., ser. LNCS, S. Ravela and A. Sandu, Eds. Springer, 2015, vol. 8964.
- [8] D. Uciński, *Optimal Measurement Methods for Distributed Parameter System Identification*. Boca Raton: CRC Press, 2005.
- [9] Z. Song, Y. Chen, J. Liang, and D. Uciński, "Optimal mobile sensor motion planning under nonholonomic constraints for parameter estimation of distributed systems," in *IEEE IROS*, 2005, pp. 3163–3168.
- [10] C. Tricaud and Y. Chen, *Optimal Mobile Sensing and Actuation Policies in Cyber-physical Systems*. Springer, 2011.
- [11] J. Haugen and L. Imsland, "Monitoring an Advection-Diffusion Process Using Aerial Mobile Sensors," *Unmanned Systems*, vol. 3, no. 3, pp. 221–238, 2015.
- [12] P. Kathirgamanathan, R. Mckibbin, and R. McLachlan, "Source Term Estimation of Pollution from an Instantaneous Point Source," *MODSIM*, vol. 6, pp. 59–67, 2002.
- [13] J. M. Stockie, "The Mathematics of Atmospheric Dispersion Modeling," *SIAM Review*, vol. 53, no. 2, pp. 349–372, 2011.
- [14] G. S. Settles, "Fluid Mechanics and Homeland Security," *Annual Review of Fluid Mechanics*, vol. 38, pp. 87–110, 2006.
- [15] S. M. LaValle, *Planning Algorithms*, 2006.
- [16] A. Atkinson, A. N. Donev, and R. D. Tobias, *Optimum Experimental Designs, With SAS*. OUP Oxford, 2007.
- [17] P. E. Gill, E. Wong, W. Murray, and M. A. Saunders, "User's Guide for SNOPT Version 7.5," Ctr. Comp. Math., UC San Diego, Tech. Rep., 2015.